Res. Rep. Fac. Eng. Mie Univ., Vol. 16, pp. 61-78 (1991)

Original Paper

Elasto-Plastic Behavior of Concrete-Filled Steel Tubular Three-Dimensional Subassemblages

Jun KAWAGUCHI, Shosuke MORINO and Chihiro YASUZAKI*
(Department of Architecture)

(Received September 17, 1991)

Three-dimensional subassemblages consisting of a concrete-filled steel tubular column and four H-shaped beams are tested under a constant axial load on the column, constant beam loads in the minor direction, and alternately repeated beam shear in the major direction simulating the earthquake loading. The specimens are designed for two types of the failure mode; shear failure of the beam-to-column connection panel, and flexural failure of the column. The paper presents the test results, and discusses the hysteretic behavior, the maximum strength, the energy dissipation capacity, and failure configuration of each specimen, comparing the test results with the results of analysis. It is concluded that the panel-failing specimens are more stable and exhibit more energy dissipation capacity compared with the column-failing specimens, the strength of the panel-failing specimen exceeds the calculated strength and reaches the strength corresponding to the column failure, although the connection panel yields in shear, and the specimen subjected to the bi-axial bending in the column becomes unstable due to excessive deformation of a doglegged shape in the minor direction.

Key Words: CFST, space frame, three-dimensional loading, bi-axial bending, maximum strength, hysteretic behavior, energy dissipation capacity, failure mode

1. INTRODUCTION

Recently mixed structures start to appear in the construction practice, which combine different types of structural systems together to develop a new type of more efficient structural system. However, the construction of such a mixed structure using new system and technique is not very easy, because of the requirements by the Building Standard Law which are specified for each of single types of structural systems separately. In other words, the Law could not follow the speed of new constructional developments, and the design standards are not yet prepared to evaluate the structural safety of such mixed structures.

The research presented here deals with the concrete-filled steel tubular (CFST) structure which is one of the popular samples of mixed structures. The CFST structures have not been often constructed mainly because of the administrative regulations stated above, but its structural characteristics have been clarified by the extensive investigations. According to Ref. [1], the first construction example of CFST structure is Severn Bridge completed in 1879 in

* NKK Corporation

England, and the first research report was by T.S. Swell in 1902 on CFST members, in which filled concrete was used as anti-corrosion material. Until 1960's, the use of CFST members was limited to a compression member, and the compression tests of concrete-filled circular tubes were conducted.

The application of a CFST member to the beam-column subjected to severe bending moment was then tried, and the investigation of its flexural behavior was done in 1970's and after. Tomii and Sakino [2~4] confirmed that CFST columns using square tube possessed sufficient strength and ductility except for those with very high axial load ratio and/or large width-thickness ratio, and presented an evaluation formula for the flexural strength of CFST members. References [5, 6] concluded from the experimental results that the compression and flexural strengths of CFST columns with rectangular tubes both exceeded the superposed strengths because of the interactive effects between steel and concrete, that is , confining effect on concrete by steel tube, and restraining effect of concrete on the local buckling of steel tube. On the other hand, it was concluded in Refs. [7] that those interactive effects were clearly observed in the columns with circular tube, but not very clear in the columns with square tube. Comparison of the test results of CFST members and pure steel members with square hollow section (SHS) showed that the limiting value of width-thickness ratio of a CFST member could be relaxed to twice the value for a SHS member, if the same deformation capacity is required [8], and that the reserved strength in a SHS member due to the strain-hardening was not necessarily observed in a CFST member, if they were designed to have the same allowable strength for the short-term loading condition [9]. The analysis of the flexural behavior of CFST members was conducted in Refs. [10] where a multi-element model for the cross-section was used with the bi-linear type stress-strain curves of steel with Bauschinger effect and the degrading type curve of concrete. Some innovations were found in Ref. [11] where filled-concrete in steel tube is confined by high-strength spiral hoops arranged inside the tube, and in Refs. [12] where the super-strength concrete is filled by the centrifugal casting method.

The researches on the beam-to-column connections in a CFST frame are separated into two groups; the researches on the form of diaphragm in the connection between a CFST column and an H-shaped steel beam, and on the connection between a CFST column and a member of different structural system. Matsui, et al. [13] investigated two types of diaphragm; through-type diaphragm with opening for concrete casting, and outside ring-type diaphragm which surrounds a CFST column without cutting it. The performance of the former type was proved to be better than that of the latter. In addition, Matsui, et al. [14] proposed side stiffener-type and emphasized its efficiency and applicability to the real practice, based on the experimental investigation. Morita, et al. investigated the method of strengthening the through-type diaphragm, and proposed formulas to evaluate the ultimate strength [15]. Innovations to prevent the local distortion of the tubular cross section have been found. Kimura, et al. proposed the use of triangular stiffeners arranged inside the tube [16], and Ito, et al. showed the efficiency of increasing the thickness of the panel portion of the tube with the longitudinal stiffeners, instead of the use of diaphragm in the beam-to-column connection [17, 18]. The use of the longitudinal stiffener was also proposed by Kimura, et al. [19], where the experiments and the analysis showed that the thickness of the tube must be limited if the longitudinal stiffeners were used. An alternative of the connection between a CFST column and an H-shaped beam without using diaphragm was shown by Nakamura, et al. [20, 21], which was composed of the end plates of the beam and long high-strength friction bolts passing through the connection panel.

As to the connection between a CFST column and a member of different structural system, the following connections have been experimentally investigated; connection with a reinforced concrete flat slab [22], connection with a steel reinforced concrete beam [23], and connection with a composite beam [24].

As stated above, the behaviors of CFST columns and of the connections with CFST columns have been extensively investigated. In addition, investigated were the bond between the concrete and the steel tube, the efficiency in concrete-filling around the connection using the through-type diaphragm, and the behavior under the fire load, which are all important in a real construction practice. However, there have been no research found on the three-dimensional behavior of a frame consisting of CFST columns under the severe earthquake, in which the column behavior under the bi-axial bending and the connection behavior under the three-dimensional loading may combinedly appear. From this point of view, three-dimensional subassemblages consisting of a concrete-filled steel tubular column and four H-shaped beams are tested under a constant axial load on the column, constant beam loads in the

minor direction, and alternately repeated beam shear in the major direction simulating the earthquake loading. The specimens are designed for two types of the failure mode; shear failure of the beam-to-column connection panel, and flexural failure of the column. The paper presents the test results, and discusses the maximum load carrying capacity, hysteretic behavior, energy dissipation capacity and the failure configuration, comparing the test results with the results of analysis.

2. EXPERIMENT

2.1 Specimen

Figure 1 is a schematic illustration of a specimen and loading condition. First, constant axial load P is applied on the top of the column, and constant vertical loads W_1 and W_2, which simulate long-term loads, are applied at the tips of short beams (beam B). A couple of anti-symmetrical, alternately repeated load Q simulating earthquake effects are applied at the tips of long beams (beam A). Experimental parameters are as follows: failure types (panel failing type or column failing type); and pattern of the long-term loads on beam B, that is, (1) no loads (W_1=W_2=0), (2) balanced loads (W_2=W_1), (3) unbalanced loads (W_2>W_1), and (4) one-side load (W_2=0). Constant bending moment about x-axis (see Fig. 1) caused by W_1 and W_2 in the case of (3) and (4) is set equal to the allowable bending moment of the specimen for long-term loading condition, calculated according to Ref. [25]. The axial load P is equal to the value of 15% of the ultimate compressive strength of the column. Table 1 shows the correspondence between the value of each parameter and the name of specimen.

Figure 2 shows the detailed shape and size of the specimen. The frame specimen consists of a CFST column (□-125x125x6) and H-shaped built-up steel beams (H-250x250x6x9) arranged in two directions. Beam-to-column connection of P-series specimen is made of steel tube (□-125x125x4.5) and that of C-series specimen is made of a box-shape built-up by welding steel plates (PL-9). Thus, the former fails in the panel shear in the connection, and latter in the column flexure. Diaphragm plates whose thickness is the same as that of the beam flange pass through the connection and have openings for concrete casting. The beams are designed so that they remain elastic until the end of the test. Materials grades of steel portion are STKR400 for steel tube and SS400 for steel plate. Table 2 shows the average values of mechanical properties obtained from the coupon test of steel and the cylinder test of concrete. The mixture of concrete is shown in Table 3. Measured dimensions of each specimen are given in Table 4.

2.2 Test Set-up

Figure 3 shows the test set-up. The specimen ① is set in the loading frame ②, and the top and bottom of the column are supported by ball-bearings ③. A steel arm ⑤ is attached to the end of each beam by high-strength bolts, and mechanical screw jacks ④ are connected to the tips of those loading arms by pins. The distance between ball bearings at the column ends is 2270 mm, and the distances between pins at the beam ends are 3600 mm and 2500 mm for the long and short beams, respectively. The horizontal movement of the specimen at the top is prevented by four horizontal braces ⑥. First, the constant axial load P is applied on the top of the specimen by a hydraulic jack ⑦. The constant vertical loads (W_1 and W_2) are applied on beam B next, and then the alternately repeated vertical loads Q are applied on beam A controlling the displacement amplitude to be prescribed value.

The procedure of alternately repeated loading on beam A is as follows: First, two cycles of the repeated load is applied with controlling the amplitude of rotation angle R to be equal to ±0.5/100 radian, and then two more cycles of the load with the amplitude of ±1/100 radian. This process is repeated with increasing the amplitude of the rotation angle R by the amount of ±1/100, after every two cycles of loading are completed. The test is terminated in general when the column can not sustain the axial load.

Figure 4 shows the position of displacement meters and measuring method of rotation angle R. Displacement meters D_1 and D_2 measure the relative displacements of column against beam A, which are placed on the measuring frame supported at the points 15 cm inside the loading points of beam A. All loads, i.e., constant axial load P,

constant vertical loads W_1 and W_2, and repeated vertical loads Q are measured by load cells 8 attached to each jack. Wire strain gauges are mounted on the steel portion of column and the beam-to-column connection panel.

2.3 Test Results

2.3.1 Hysteretic Behavior

Figure 5 shows the relations between the load Q and the rotation angle R of all specimens. Specimens with numerals 11, 20 and 31 in their names are tested under the three-dimensional loading condition, and the columns of specimens with the numerals 20 and 31 are subjected to the bi-axial bending.

P-series Tests of SCP00 and SCP11 of which columns are subjected to uni-axial bending were terminated because of short stroke of the screw jacks. Tests of SCP20 and SCP31 were terminated when the specimens became unstable showing doglegged deformation in the y-z plane. Deformation capacity of SCP00 is large, and also SCP11 whose column is subjected to the uni-axial bending has large deformation capacity. Though SCP20 and SCP31 show less deformation capacity, the loading cycles of rotation angle R = ±4/100 are completed. Strength deterioration due to the repeated loading are not large in any specimen, and the hysteresis loops are stable until the end of the test. Compared with the corresponding C-series specimen, the strength at the same rotation angle is lower, but the deformation capacity is larger.

C-series The test of SCC00 and SCC11 with columns subjected to the uni-axial bending were terminated when the specimens could not sustain the axial load. Tests of SCC20 and SCC31 whose columns were subjected to the bi-axial bending were terminated when the unstable doglegged deformation appeared in y-z plane. Energy dissipation capacity becomes larger in the order of SCC20, SCC31 and SCC11. The strength deterioration after the maximum strength becomes severer in the order of SCC31, SCC11 and SCC00. SCC20 did not show the strength deterioration because before it appeared the test was terminated due to the instability in the y-z plane. The unstable deformation and the strength deterioration of specimens tested under the three-dimensional loading condition were observed when the rotation angle R reached ±3/100 to ±4/100.

Strains at the beam-to-column connection panel The relations between the repeated load Q and the diagonal strain ε_p obtained from the wire strain rosette gauges mounted on the connection panel are shown in Fig. 6. The panels of P-series specimens yield and show stable hysteresis loops, which means that the input energy is dissipated by the panel deformation in the case of P-series. Strains of C-series specimens stay in the elastic range until the end of the test.

2.3.2 Failure Modes

Figure 7 shows the relations between the load Q and the longitudinal strain ε_c of the column, and Fig. 8 shows the relations between Q and the horizontal displacement D_3 along the x-axis at the beam-to-column connection. Deformed configurations of the specimens at the collapse state are schematically illustrated in Fig. 9.

P-series Two failure types are observed in this series. In the first type observed in SCP00 and SCP11, anti-symmetrical shear deformation of the beam-to-column connection panel appears (Fig.6 (a) and (b)), and plastic hinges form at the ends of both the upper and lower columns (Fig. 7 (a)). This type shows the anti-symmetrical S-shape deformation as shown in Fig. 9 (a) at the early stage of loading, and then shows the accumulation of D_3 in one direction in the range of large deformation. The tests of these specimens were terminated because of the shortage of the jack stroke, although the column was still able to sustain the axial load. The other type is almost the same as the former type during the small deformation, but in the large deformation range, the local buckling occurs in the three surfaces of the lower column (Fig. 7 (b)), the shear deformation of the panel accumulates in one-direction (Fig. 6 (c) and (d)), and unstable doglegged deformation in y-direction appears as illustrated in Fig. 9 (c). However, the horizontal displacement accumulations in x-direction as seen in Fig. 8 (c) and (d) are not observed.

C-series Two types of the failure mode are also observed in C-series. In the first type, the local buckling occurs at the ends of both the upper and lower columns (Fig. 7 (c)) and the symmetrical doglegged deformation of the column

appears during the small deformation. Then, the horizontal displacement accumulation at the connection as illustrated in Fig. 9 (b) occurs (Fig. 8(e) and (f)), and the column becomes unstable to sustain the axial load. This type is observed in SCC00 and SCC11. The other type observed in SCC20 and SCC31 shows the similar behavior as the former type during the small deformation, but the unstable doglegged deformation in y-direction appears in the large deformation range as illustrated in Fig. 9 (c).

3. DISCUSSIONS

3.1 Elastic Stiffness and Ultimate Strength

3.1.1 Elastic Stiffness

Deformation obtained from the test contains flexural and shear deformations of columns and beams, and shear deformation of the beam-to-column connection panel. Thus, the calculation of the elastic stiffness must consider these effects. The second elastic stiffness after the filled-concrete cracks is also calculated as follows. Strictly speaking, if the moment at the column end exceeds the concrete cracking moment M_c (Ref. [26]), the column shifts to the non-prismatic member and the distribution of rigidity along the length becomes non-uniform. The neutral axis of the section in which concrete cracks moves according to the load level. However, these effects are all neglected to simplify the calculation, and the second stiffness after the concrete crack occurs is calculated by assuming that the column is still prismatic with the cracked section at the column end in which the stress at the extreme compressive fiber reaches $F_c/3$, and the effective area of concrete exists only in the compressive side of the neutral axis, where F_c denotes the cylinder strength of concrete.

3.1.2 Ultimate Strength

The ultimate values of the panel moment ${}_JM_U$ and the column end moment ${}_CM_U$ corresponding to the ultimate shear strength of the connection panel and the ultimate flexural strength of the column are calculated based on Ref. [25] for P- and C-series specimens, and they are converted to the load at the tip of beam A by Eqs. (1) and (2), respectively.

$$ {}_cQ_{max} = {}_CM_U \cdot (h/h') \tag{1} $$

$$ {}_pQ_{max} = {}_JM_U \cdot (h/h')/2 \tag{2} $$

where, ${}_pQ_{max}$: the maximum load at the tip of beam A based on the ultimate shear strength of the connection panel,

${}_cQ_{max}$: the maximum load at the tip of beam A based on the ultimate flexural strength of the column,

${}_JM_U$: the ultimate moment acting around the panel failing in shear,

${}_CM_U$: the ultimate flexural strength of the column,

h : half length of the column, measured between the center of the connection panel and the ball bearing at the column end, and

h' : half clear length of the column, measured between the face of the beam and the ball bearing at the column end (h – (half the panel height)).

The effect of bi-axial bending to the ultimate strength is not considered in these calculations.

3.2 Discussions

3.2.1 Ultimate Strength

Figure 10 shows the envelop curves obtained from the hysteresis loops of the specimens. Dotted lines show the elastic stiffness calculated in 3.1.1, and solid lines and chain lines show the ultimate strengths obtained from the flexural strength of the column and the shear strength of the panel, respectively, calculated in 3.1.2.

P-series Though design calculation was done based on Ref. [25] and the shear yielding of the connection panel have preceded the flexural yielding of the column, the maximum strength of all specimens exceeds the ultimate strength corresponding to the shear strength of the panel, and reaches the ultimate strength corresponding to the column flexural strength, except for SCP20. Therefore, it may be said that the beam-to-column connection panel was confined by beam B and steel tube, and its maximum strength rose, although the panel yielded in shear. SCP20 subjected to one side loading on beam B shows a little smaller strength compared with other specimens in P-series, but the effect of the bi-axial bending of this series is not remarkable. This trend is also observed in SCC31 which is subjected to the same flexural pattern in y-direction as SCP20. Pattern of the three-dimensional loading may affect the maximum strength.

C-series Calculated ultimate strength shows good evaluation of the maximum strength obtained in the tests. All specimens reach the calculated strength based on the ultimate flexural strength of the column under the uni-axial bending. Since the maximum strength of the specimen subjected to the bi-axial bending reaches the calculated uni-axial bending strength, the bi-axial bending and the three-dimensional loading may not much affect the maximum strength.

3.2.2 Hysteretic Behavior

Comparison of the hysteresis loops of P-series specimens with those of the corresponding specimens in C-series shows that the strength deteriorations after the maximum strength in P-series is less than in C-series, and the deformation capacity of the former is larger; P-series are more stable than C-series. Three-dimensional loading with the uni-axial bending in columns (SCP11 and SCC11) seems not to give any effects to P-series specimen, but decreases the deformation capacity of C-series specimen. This is because that the column of C-series specimen deforms in a doglegged shape and the horizontal displacement of the connection panel (D_3 in Fig. 8) accumulates in one direction, which causes large PΔ moment in the column. The effects of the bi-axial bending appear remarkably: The deformation capacity of the specimens subjected to the bi-axial bending (SCP20, SCP31, SCC20 and SCC31) is quite small in both series, compared with the specimens subjected to the uni-axial bending. In these specimens, the bending axis rotates with the repeated loading, and this causes the earlier local buckling of the steel tube which leads to the less deformation capacity.

3.2.1 Failure Modes

C-series specimens subjected to the bi-axial bending show the unstable doglegged deformation in the y-direction after the local buckling in the column occurs, and the horizontal displacement of the connection accumulates causing large PΔ moment. On the other hand, P-series specimens show the symmetrical S-shape deformation, and the horizontal displacement of the connection does not become very large. Therefore, P-series specimens show more stable failure modes than C-series specimens.

4. CONCLUDING REMARKS

New findings obtained from the experimental study on the elasto-plastic behavior of three-dimensional concrete-filled steel tubular subassemblages are as follows:

(1) The maximum strengths of P-series specimens are almost the same, and the effects of neither the three-

dimensional loading nor the bi-axial bending are recognized. On the other hand, both the three-dimensional loading and the bi-axial bending reduce the maximum strengths of C-series specimens.

(2) The maximum strengths of P-series specimens exceed the calculated ultimate strengths corresponding to the beam-to-column connection panel failure, and reach the ultimate strengths based on the column flexural failure. Thus, there are some cases that the strength formulas in the current standards give conservative evaluation to the ultimate strength.

(3) P-series are more advantageous than C-series as to the deformation and the energy dissipation capacities.

(4) Specimens subjected to the bi-axial bending show the unstable doglegged deformation in y-direction, which is not very clear in P-series specimens.

(5) Only the bi-axial bending decreases the deformation capacity in P-series. On the other hand, not only the bi-axial bending but also the three-dimensional loading decrease the deformation capacity in C-series.

(6) Beam-to-column connection panels of P-series specimens yield and deform by shear, but the strength increases after the panel yields, and the plastic hinge forms in the column.

(7) Two types of the failure mode are obtained in each series. All C-series specimens and P-series specimens subjected to the bi-axial bending show the doglegged deformation of the column. P-series specimens subjected to the uni-axial bending show stable behavior and can sustain the axial load until the end of the test.

Acknowledgments

The authors wish to express their sincere gratitude to Messrs. Toshiya Nomura (Mie University) and Yasunori Masuda (Mitsuhashi Architects), who helped in the experiments of this investigation.

References

[1] M. Tomii and K. Sakino: A State of Art Report on Concrete Filled Steel Tube Structures, Concrete Journal, Vol.13, No 2, 1974, pp. 26-40.

[2] M. Tomii, K. Sakino and F. Fujiwara: Experimental Study on the Concrete-Filled Steel Tubular Beams and Beam-Columns under Horizontal Loading (Part 1, 2, 3, 4 and 5), Abstracts, Annual Meeting of Architectural Institute of Japan (A. I. J.), 1971.11, pp. 749-752; 1972.10, pp. 1093-1094; 1976.10, pp. 1539-1540; 1978.9, pp.1899-1900.

[3] M. Tomii, K. Sakino and K. Kiyohara: Experimental Study on the Concrete-Filled Steel Tubular Beam-Columns Subjected to Constant Axial Load and Bending Moment, Abstract, Annual Meeting of A. I. J. , 1978.9, pp. 1901-1902.

[4] K. Sakino and M. Tomii: Study on the Ultimate Strength of Concrete-Filled Steel Tubular Beam-Columns, Abstract, Annual Meeting of A. I. J. , 1981.9, pp.2127-2128.

[5] Y. Saito, I. Yamaguchi, T. Matsutani, A. Kadono, H. Matsumura, T. Yamaguchi, H. Ueda, M. Nakajima, S. Sawada, T. Sato, Y. Nakamura, Y. Kurose, Y. Watanabe and K. Konno: A Study on the Behavior of Concrete-Filled Steel Tubular Columns (Part 1, 2, 3, 4 and 5), Abstracts, Annual Meeting of A. I. J. , 1989.10, pp. 1613-1622.

[6] B. Kato, H. Akiyama, H. Furukawa and I. Nishiyama: Experimental Study on the Concrete-Filled Steel Tubular Beam-Column Subjected to Horizontal Loading (Part 2 and 3), Abstracts, Annual Meeting of A. I. J. , 1976.10, pp. 1535-1536; 1977.10, pp. 1473-1474.

[7] K. Takada, T. Matsutani, M. Nakajima, K. Okada, T. Ide, T. Sakamoto, N. Iida, S. Sawada, H. Ueda, H. Nose, J. Ishida, M. Shinoda, H. Kamisawa, K. Katagihara and Y. Kuroki: Experimental Studies of Super-Highrise Building with Concrete-Filled Steel Tubular Columns (Part 5, 6, 7, 8, 9, 10 and 11), Abstracts, Annual Meeting of A. I. J. , 1988.10, pp. 1405-1410; 1989.10, pp. 1603-1610.

[8] M. Kimura, H. Okimoto, Y. Nakayama and K. Ishida: Behavior of Concrete-Filled Square Steel Columns under Shear Bending (Part 1 and 2), Abstracts, Annual Meeting of A. I. J. , 1986.8, pp. 1413-1416.

[9] T. Takeda, K. Kohata, Y. Takahashi and T. Tada: Shear Bending Tests of Square Steel Columns and Concrete-Filled Square Steel Columns under High Axial Load, Abstract, Annual Meeting of A. I. J. , 1987.10, pp. 1285-1286.

[10] M.Yamada, H. Kawamura, K. Shiotani, M. Yamano and N. Sugano: Study on Elasto-Plastic Flexural Deformation Behavior of the Concrete-Filled Steel Tubular Columns under the Axial Load (Part 1, 3, 5, 6, 7 and 11), Abstracts,

Annual Meeting of A. I. J. , 1975.10, pp. 1205–2106; 1976.10, pp. 1537–1538; 1977.10, pp. 1481–1482; 1978.9, pp. 1889–1890; 1979.9, pp. 1653–1654; 1981.9, pp. 2129–2130.

[11] T. Nagashima, S. Sugano, H. Sawada and T. Kei: An Experimental Study on Behavior of Concrete–Filled Steel Tubular Columns under Cyclic Loading Axial Load, Abstract, Annual Meeting of A. I. J. , 1989.10, pp. 1601–1602.

[12] T. Okamoto, T. Maeno, T. Kutoku, K. Kaneta and H. Nishizawa: An Experimental Study on Rectangular Steel Tube Columns Infilled with Ultra High Strength Concrete, Abstracts, Annual Meeting of A. I. J. , 1989.10, pp. 1611–1612; 1990.10, pp. 1039–1040.

[13] C. Matsui and K. Kondo: Study on the Beam–to–Column Connections of the Concrete–Filled Steel Tubular Columns and the H–Shaped Steel Beams, Abstract, Annual Meeting of A. I. J. , 1989.9, pp. 1661–1662.

[14] C. Matsui, A. Kawano, C. Lee and H. Matsumura: New Connections with H–Shaped Beam to Steel Square Tubular Column (Part 1 and 2), Abstracts, Annual Meeting of A. I. J. , 1989.10, pp. 1599–1560; 1990.10, pp. 1087–1088.

[15] K. Morita, Y. Yokoyama, Y. Kawamata and H. Matsumura: Structural Behaviors of Concrete–Filled Tubular Column–to–Steel Beam Connections Reinforced with Inner Open Diaphragm (Part 1,3 and 4), Abstracts, Annual Meeting of A. I. J. , 1989.10, pp.1643–1644; 1990.10, pp. 1075–1078.

[16] M. Kimura, H. Ohta, T. Kashimura, M. Ohta, K. Mogami and K. Nogami: Study on the Connections of Concrete–Filled Tubular Steel Columns, Abstract, Annual Meeting of A. I. J. , 1988.10, pp. 1389–1390.

[17] S. Ito, T. Miyao, K. Morita, K. Endo and Y. Kawai: Strength of Joints of Concrete–Filled Steel Column to Steel Beam, Abstract, Annual Meeting of A. I. J. , 1989.10, pp. 1639–1640.

[18] T. Miyao, S. Ito, K. Endo, K. Morita and Y. Kawai: Strength of New Type Concrete–Filled Tubular Column–to–Beam Joints, Abstract, Annual Meeting of A. I. J. , 1990.10, pp. 1085–1086.

[19] K. Okamura, M. Kimura, T. Kashimura, H. Ohta, M. Ohta and K. Hatanaka: Development of the Connections of Concrete–Filled Tubular Steel Columns (Part 1), Abstract, Annual Meeting of A. I. J. , 1989.10, pp. 1647–1648.

[20] C. Matsui, K. Tsuda, N. Nakamura, M. Sawada: Experimental Study on Concrete–Filled Steel Column– Steel Beam Joints Fastened with Long–Through Bolts, Abstract, Annual Meeting of A. I. J. , 1988.10, pp. 1395–1396.

[21] N. Nakamura, K. Inoue, M. Tada, H. Matsumura, H. Kamura and M. Sawada: Study on Concrete–Filled Steel Column–H Shaped Beam Joints with End Plate Reinforced Rib Plate (Part 1 and 2), Abstracts, Annual meeting of A. I. J. , 1990.10, pp. 1089–1092.

[22] N. Mitsui, K. Endo, K. Kosugi, T. Yamada: Vertical and Horizontal Loading Tests on R/C Flat–Slab to Concrete Filled Tubular Column Connection (Part 1 and 2), Abstracts, Annual Meeting of A. I. J. , 1988.10, pp. 1391–1394.

[23] M. Kimura, H. Ohta, T. Kashimura, S. Abe, O. Ishii and H. Ohta: On The Behavior of Beam Ends Connected to Concrete–Filled Tubular Steel Columns, Abstract, Annual Meeting of A. I. J. , 1988.10, pp. 1401–1404.

[24] H. Okumura, K. Morita M. Teraoka, Y. Kato, K. Tanaka, T. Fujiwara, K. Hayashi and H. Orimo: Experimental Study on The Structure of Concrete–Filled Square Tubular Column with Composite Beam Using Inner Diaphragm (Part 1 and 2), Abstracts, Annual Meeting of A. I. J. , 1990.10, pp. 1081–1084.

[25] Architectural Institute of Japan: Standard for Structural Calculation of Steel Reinforced Concrete Structures, A.I.J. ,1987.

[26] Architectural Institute of Japan: AIJ Standard for Structural Calculation of Reinforced Concrete Structures, A.I.J., 1985.

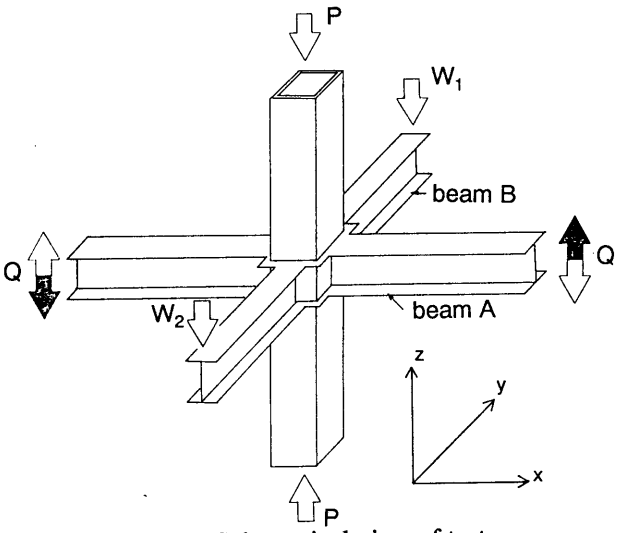

Fig. 1 Schematical view of test

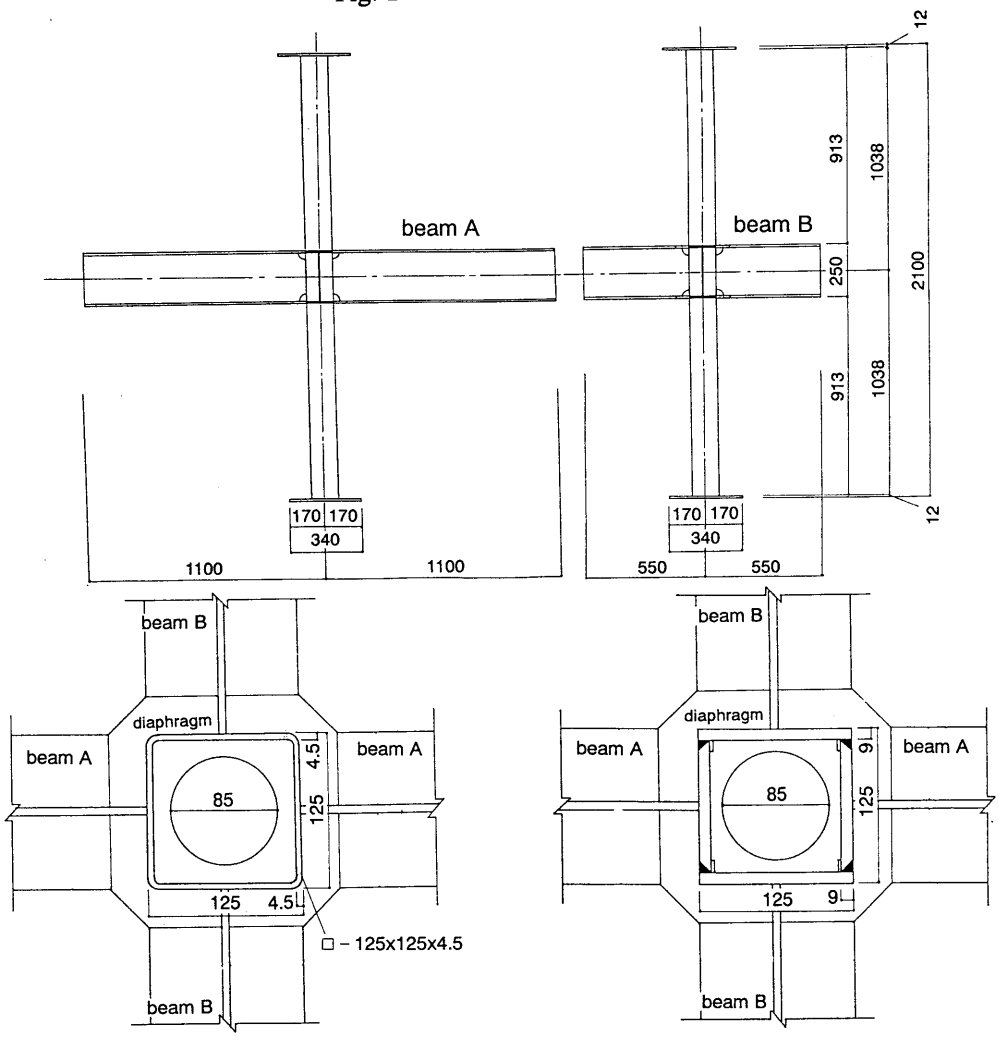

Fig. 2 Details of specimen

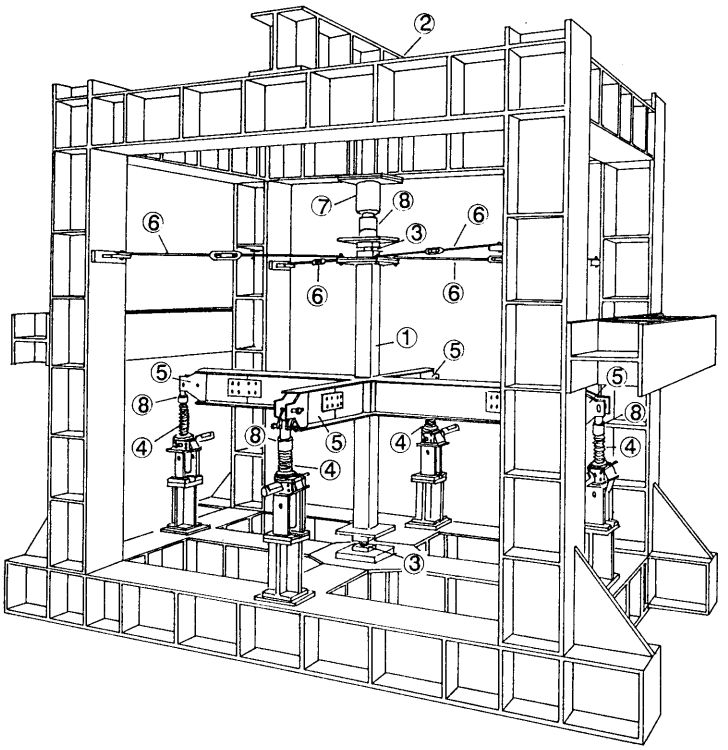

Fig. 3 Test set-up

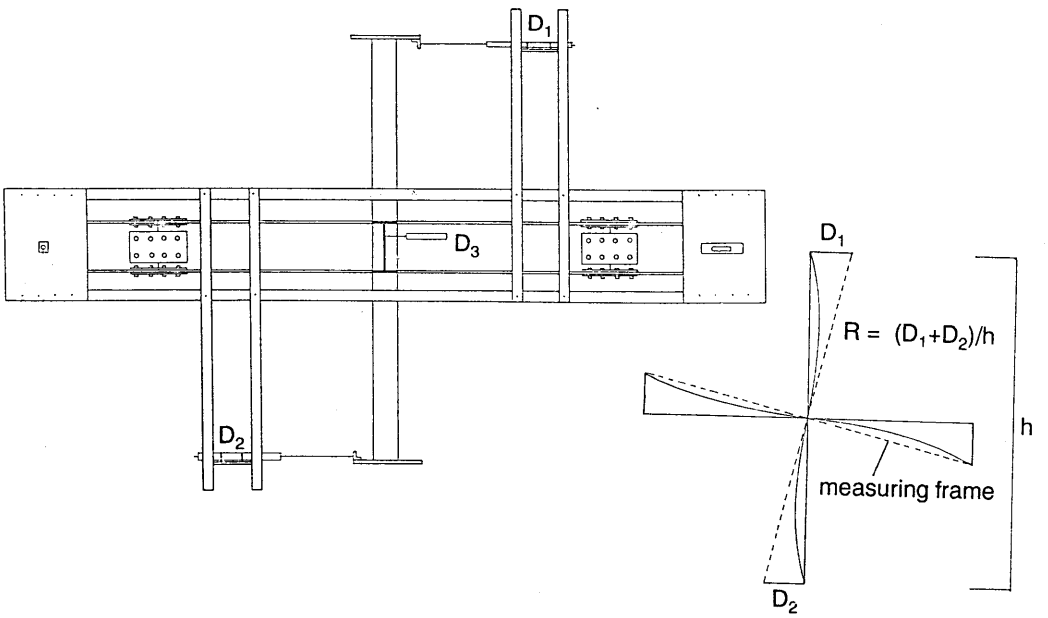

Fig. 4 Measuring system

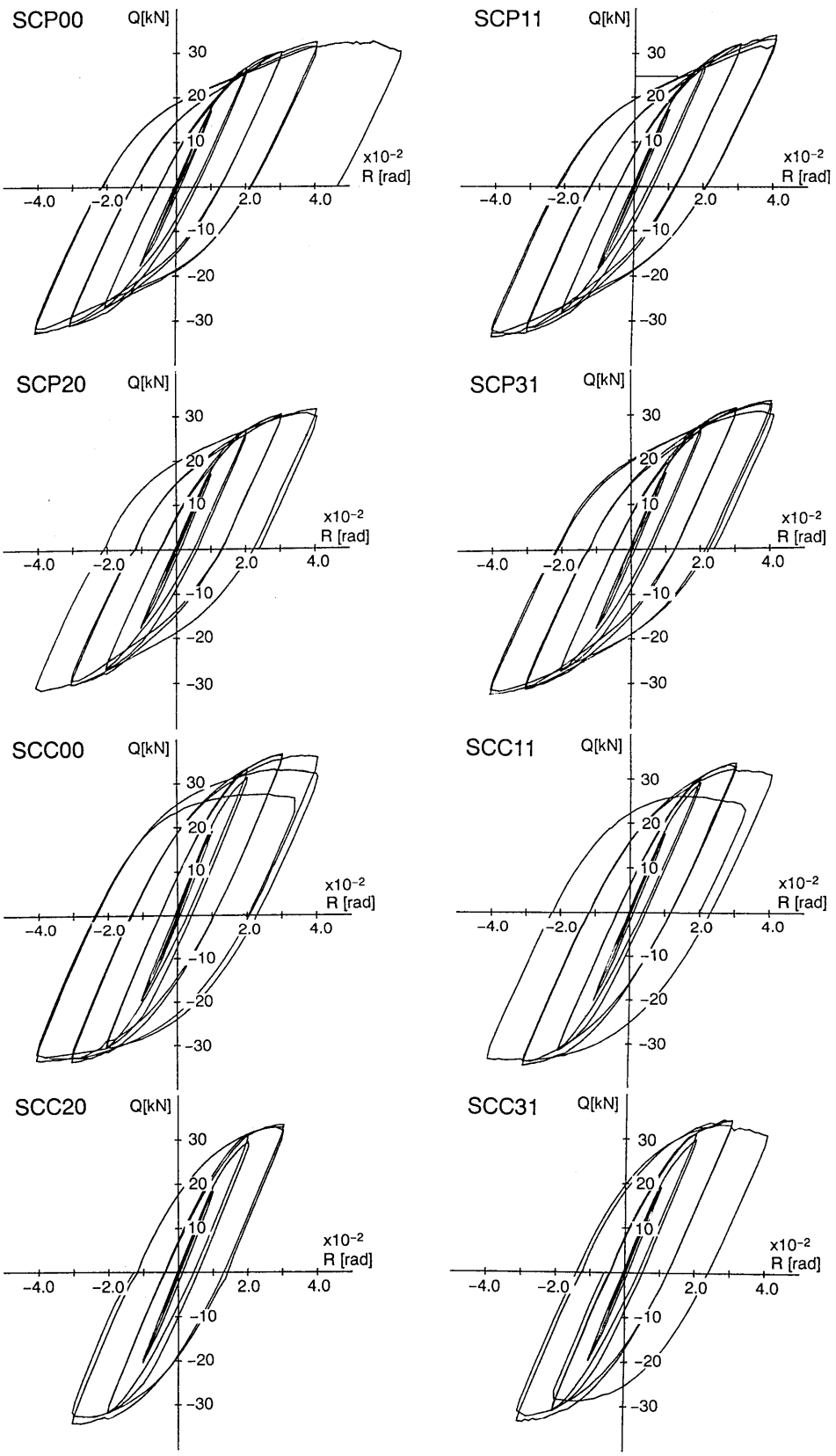

Fig. 5 Relations between load Q and rotation angle R

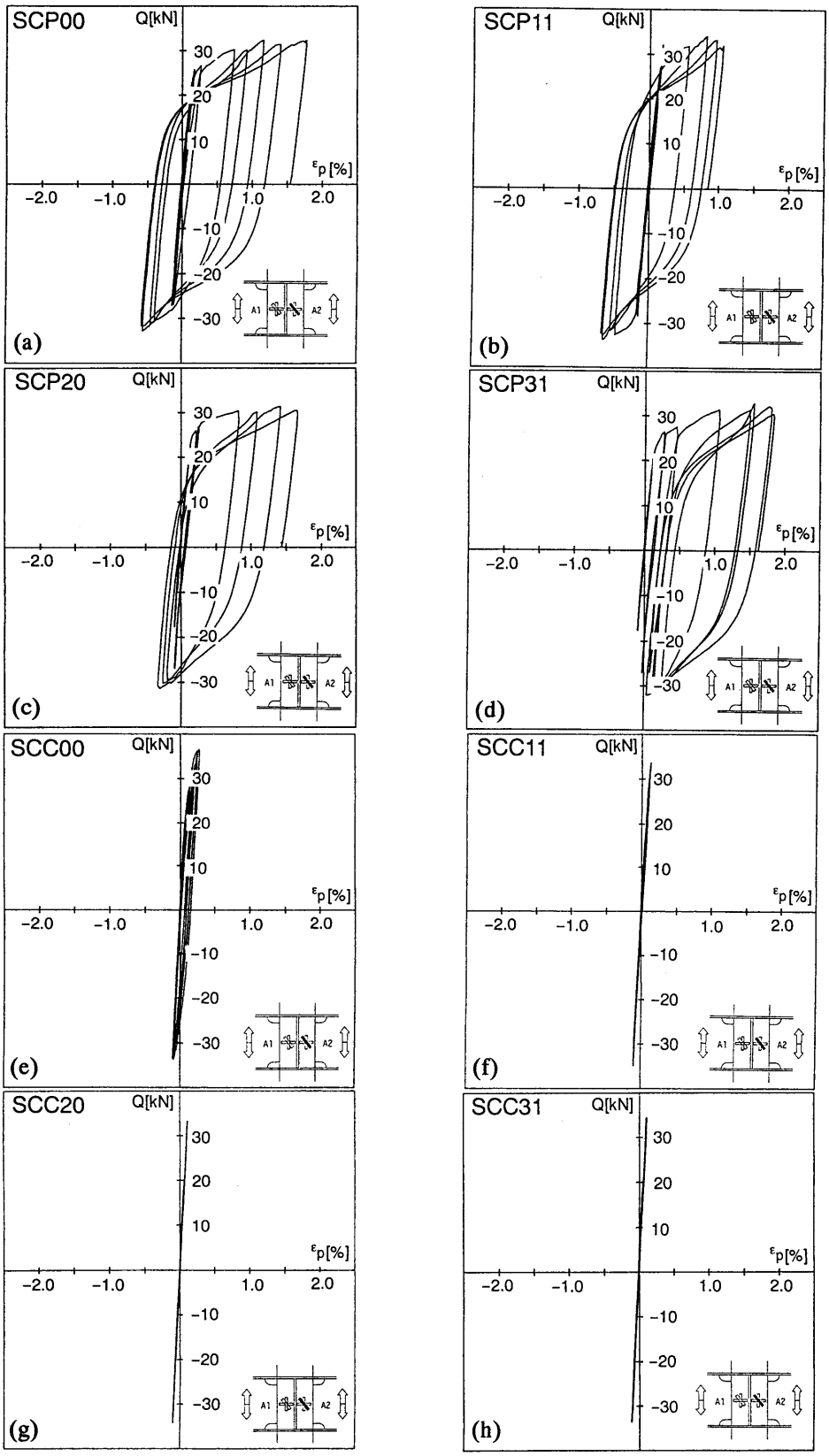

Fig. 6 Relations between load Q and strain of panel ε_p

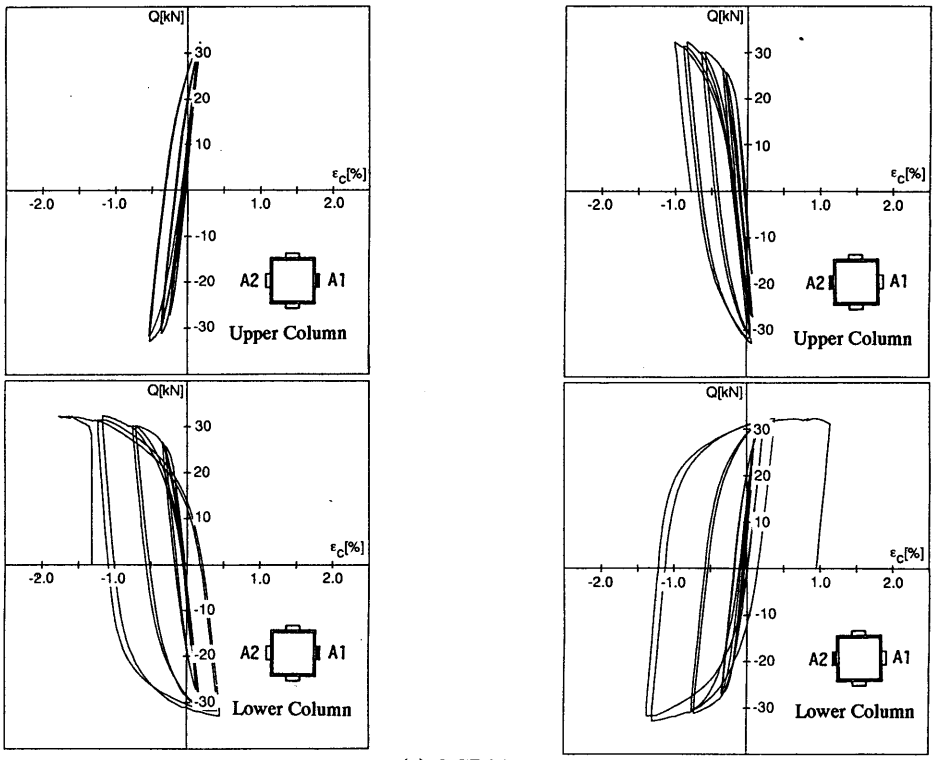

(a) SCP00

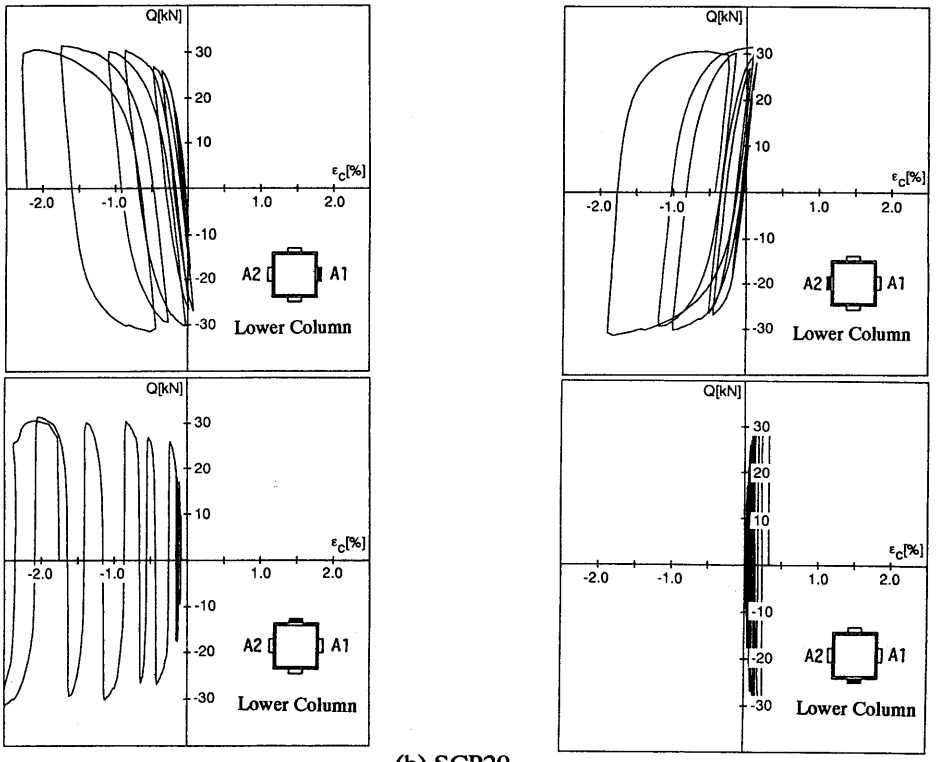

(b) SCP20

Fig. 7 Relations between load Q and strain of column ε_c

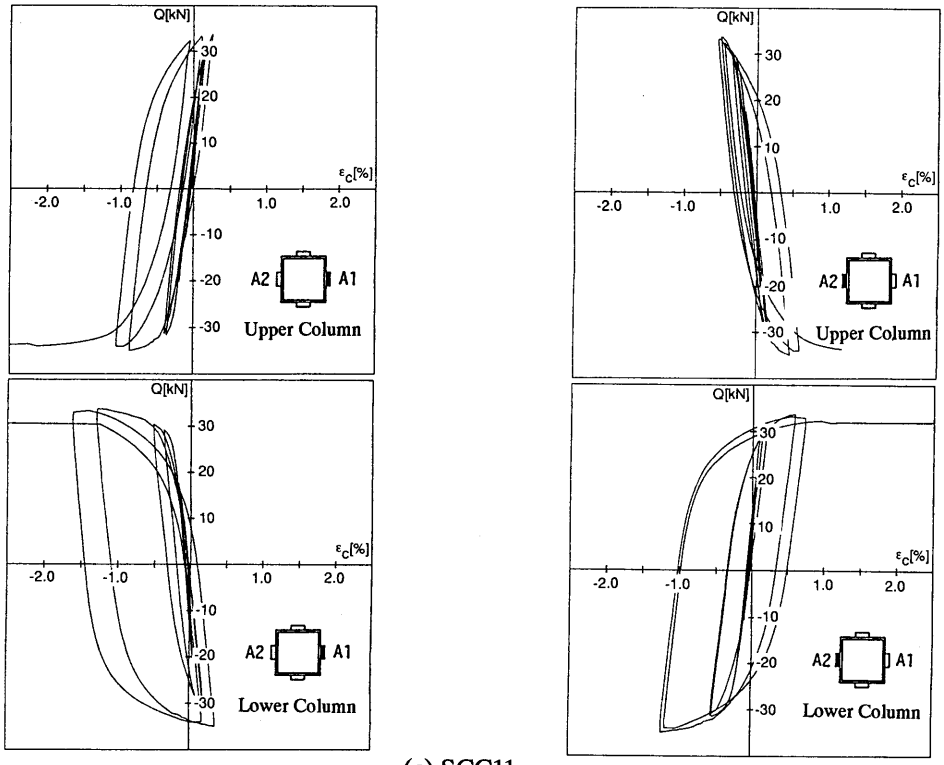

(c) SCC11

Fig. 7 Relations between load Q and strain of column ε_c (continued)

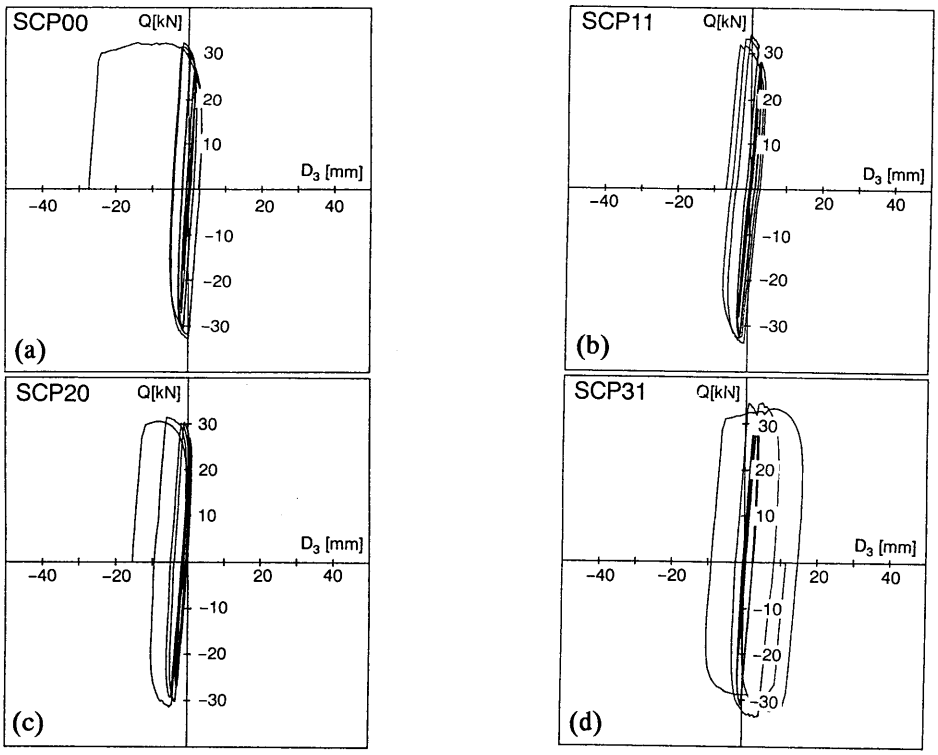

Fig. 8 Relations between load Q and horizontal displacement of connection D_3

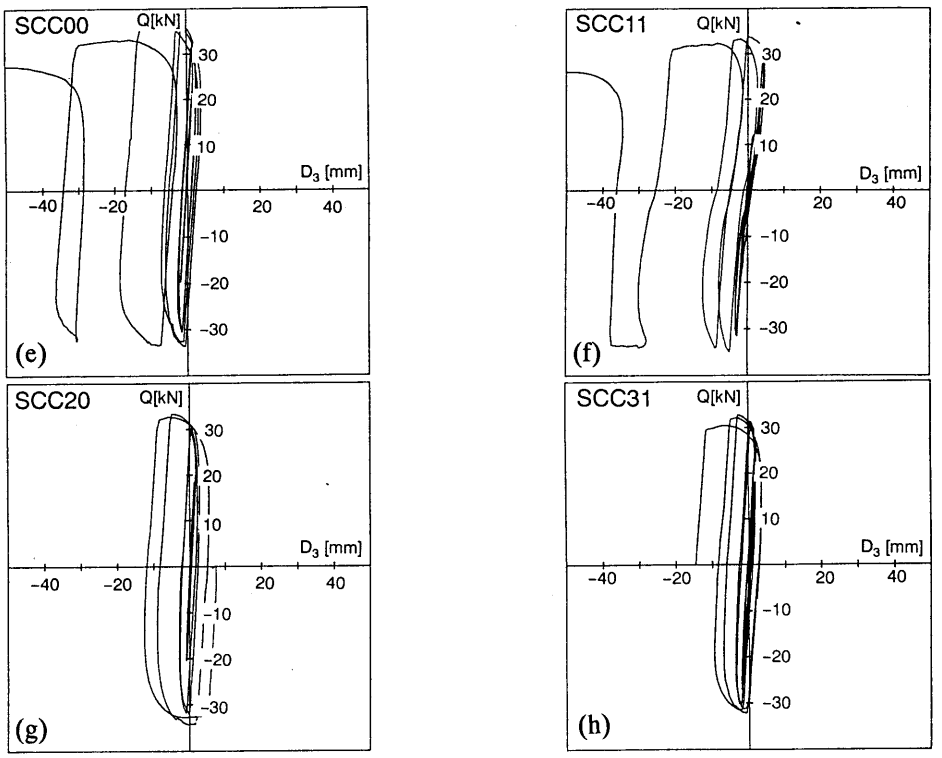

Fig. 8 Relations between load Q and horizontal displacement of connection D_3 (continued)

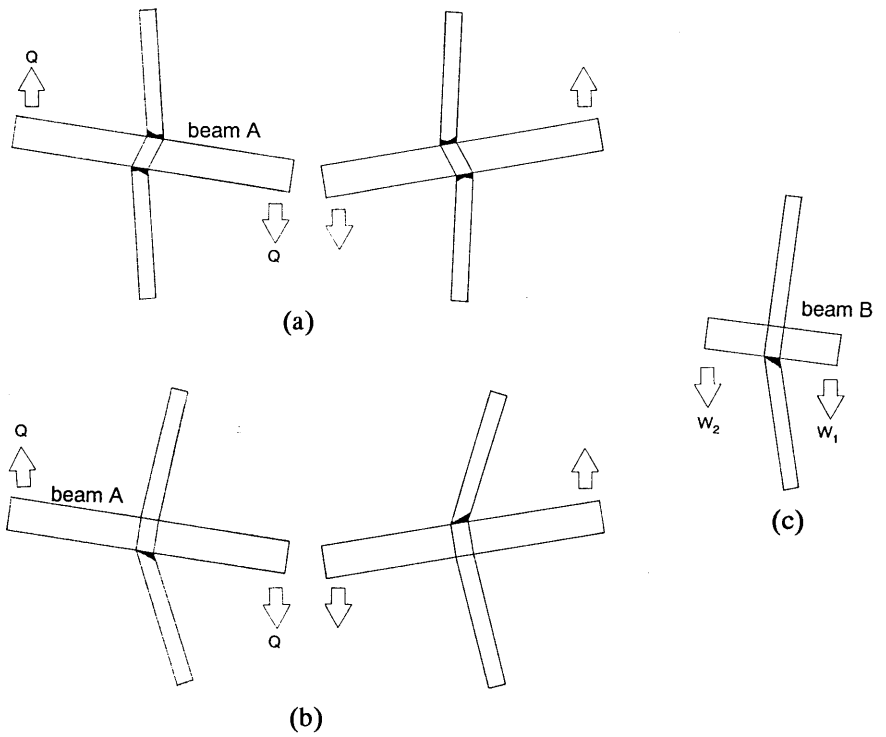

Fig. 9 Failure modes

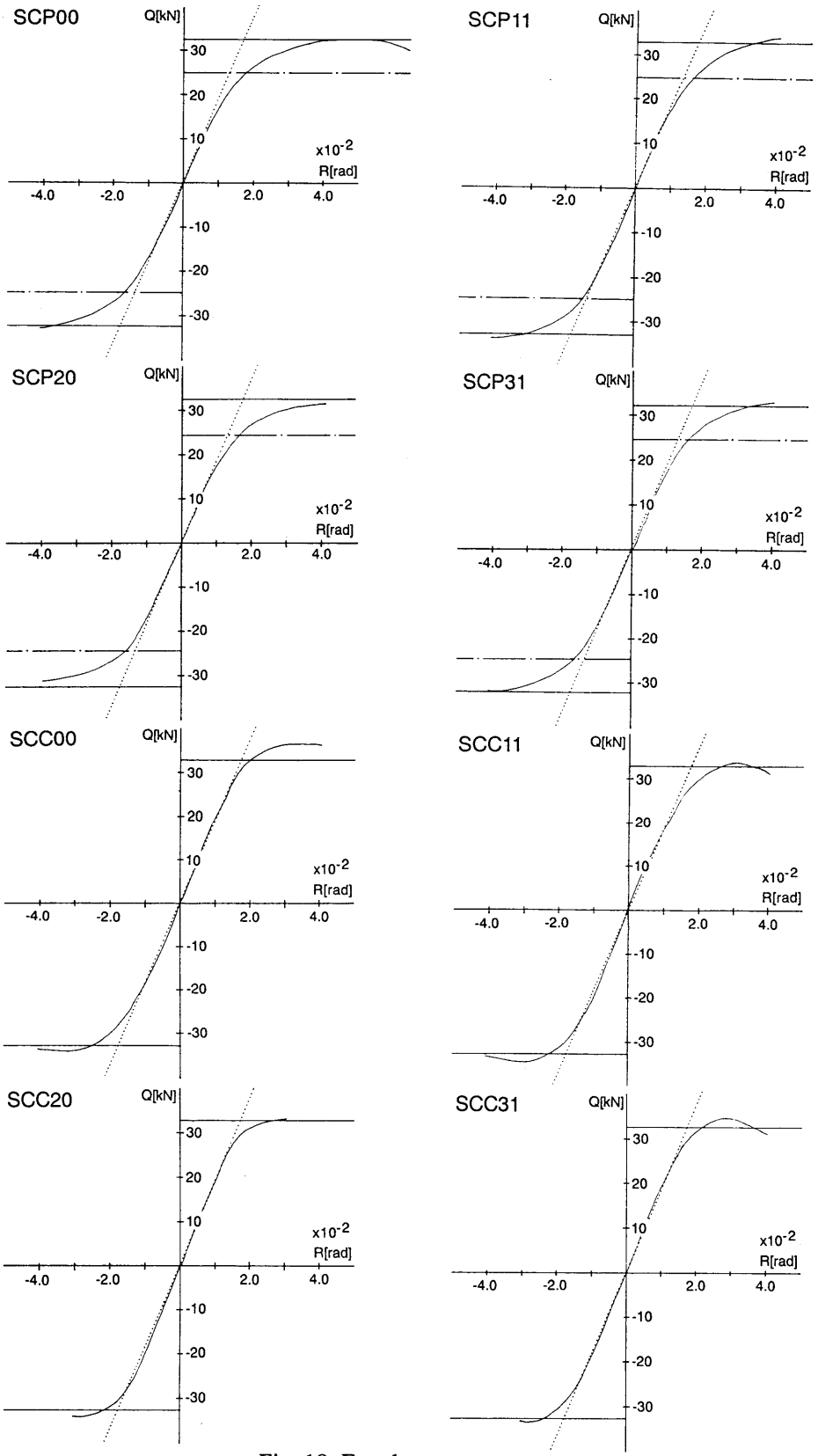

Fig. 10 Envelop curves

Table 1 Experimental parameters

Specimen	W_1, W_2 (kN)	Failure type
SCP00	0, 0	panel
SCP11	9.8, 9.8	
SCP20	21.0, 0	
SCP31	31.0, 9.8	
SCC00	0, 0	column
SCC11	9.8, 9.8	
SCC20	21.0, 0	
SCC31	31.0, 9.8	

Table 2 Mechanical properties of material

(a) Steel

	σ_y	σ_t	e
□-125x125x6	394.9	479.7	12.5
□-125x125x4.5	407.7	518.1	12.4
PL-9	268.8	373.1	29.6

NOTES:

σ_y : yield stress (N/mm^2)

σ_t : tension strength (N/mm^2)

e : elongation (%)

(b) Concrete

specimen	SCP00	SCP11	SCP20	SCP31	SCC00	SCC11	SCC20	SCC31
F_c	17.42	20.25	18.96	17.38	19.27	19.51	20.04	19.82

NOTES:

F_c : cylinder strength (N/mm^2)

Table 3 Mix proportion of concrete

F_c	G_m	SL	W/C	W	C	a	S/A	S	G	AE
21	15	18	66.5	184	277	2	50	920	949	1.94

NOTES:

F_c : cylinder strength (N/mm^2)

G_m : maximum size of course aggregate (mm)

SL : slump (cm)

W/C : water-cement ratio by volume (%)

W : water content per unit volume of concrete (kg/m^3)

C : cement content per unit volume of concrete (kg/cm^3)

a : air content (%)

S/A : sand-aggregate ratio by volume (%)

S : sand content per unit volume of concrete (kg/m^3)

G : gravel content per unit volume of concrete (kg/m^3)

AE : AE agent content per unit volume of concrete (kg/m^3)

Table 4 Measured dimensions [mm]

specimen	b_c	t_c	b_p	h_p	t_p	l_b	h	h'
SCP00	125.04	5.74	124.90	230.71	4.25	1802.0	1133.8	1009.3
SCP11	124.96	5.74	124.53	230.98	4.25	1800.5	1133.6	1009.3
SCP20	125.00	5.74	124.52	232.00	4.25	1804.5	1132.5	1007.6
SCP31	125.01	5.74	124.56	231.93	4.25	1802.5	1133.8	1008.9
SCC00	125.00	5.74	124.77	231.61	8.80	1800.0	1133.4	1005.6
SCC11	124.95	5.74	124.70	230.79	8.80	1800.0	1133.4	1009.0
SCC20	124.99	5.74	124.95	231.23	8.80	1803.0	1132.1	1007.5
SCC31	125.05	5.74	124.59	230.48	8.80	1799.0	1132.7	1008.4

NOTES:

b_c : width of column

t_c : thickness of column

b_p : width of panel

h_p : height of panel

t_p : thickness of panel

l_b : half length of beam

h : half length of column

h' : half clear length of column